

SCEC 2006 Research Annual Report of Research by Michele Cooke¹ and Andrew Meigs²

¹Geosciences Department, University of Massachusetts, Amherst, MA, 01003

²Department of Geosciences, Oregon State University, Corvallis, OR, 97331

*REFINEMENT OF COMMUNITY FAULT MODEL ALTERNATIVES USING
MECHANICAL MODELS OF DEFORMED GEOLOGIC MARKERS*

Cooke and Meigs have been funded for the past four years to integrate geologic data and mechanical models to validate the Community Fault Model (CFM) and explore alternative models. In this last year of SCEC, we finalized our methodology, refined our interpretations, and submitted papers to Geophysical Research Letters and the Bulletin of the Seismological Society of America that present the details of our research. We developed a methodology in which a range of model fault configurations and concomitant uplift can be simply tested against geologic data. Our goal throughout this project has been to validate fault topology in the CFM and provide alternative topologies for those parts of the CFM in the LA Basin where models and data do not fit well. CFM validation is a critical step in the delivery of SCEC2 community products to groups within SCEC and other users.

The project has funded and promoted a number of students in the past 4 years including Ashley Griffith and Scott Marshall at UMass and Seth Carpenter, Sam VanLaningham, Della Fawcett (an undergraduate and 2005 SCEC SURE Intern) at OSU. These individuals made substantial contributions to this project.

Comparison of model and geologic uplift rate patterns

Model-data compatibility was evaluated on the basis of structural trend, spatial variation in rates and location of major structures (i.e. near surface folds). Whereas the geological cross-sections capture the structure of the shelf of the northern LA basin in detail, Poly3D Boundary Element Method (BEM) models produce regions of uplift and subsidence that are controlled by fault geometry, connectivity, interaction of closely spaced faults, and contraction rate. It is unreasonable, therefore, to expect that the BEM models will match the geological data on the scale of the fine details of the structures. Furthermore, uncertainties associated with compaction, age, and paleotopography may influence the details of the geologic structural relief. Regions of uplift and subsidence produced by BEM models should, however, capture the major regions of geologic uplift and subsidence across the northern LA basin. A key feature, for example, that should result from the models is the central trough of the LA basin (Fig. 1). To the east of the San Gabriel River, models are expected to accurately mimic the location and extent of the structural highs associated with the Coyote and Santa Fe Springs anticlines and the structural low represented by the La Habra syncline. West of the San Gabriel River the Elysian Park anticlinorium, including the Las Cienegas monocline, extends to the Newport-Inglewood fault (Fig. 1) and has greater structural and topographic relief the Santa Fe and Coyote anticlines.

Methods

Structural relief (rock uplift) of key marker beds relative to the undeformed axis of the Los Angeles basin (LAB) provides geologic constraint of vertical motion related to faults. Three marker beds, the Repetto and Pico Members of the Fernando Formation (~4.95 and 2.9 Ma, respectively) and the base of Quaternary units (~1.4 Ma), are present in numerous wells across the ~50 km northern LAB of this study (Fig. 2). Data from these wells were integrated in cross-sections across the major structures. Rock uplift for each stratigraphic marker was measured,

and rock uplift rate calculated by dividing uplift by marker age. Contour maps of rock uplift and uplift rate serve to constrain the spatial pattern of rock uplift and rock uplift rate in time and space (Fig. 2).

Fault interaction using the BEM models is driven by remote contraction taken from geodetic studies of the region. Faults are freely slipping and respond to both remote contraction and slip along nearby structures. Comparison of model deformation under various geodetically determined tectonic loading indicate that north-south contraction of 100 nanostrain/yr with negligible east-east strain (Argus et al., 2005) best matches slip style of faults within the basin (Griffith and Cooke, 2005).

Key Findings

1. Fit between CFM-based model uplift patterns and geologic folds is good to the east of the San Gabriel River (Fig. 3a). For example, the uplift pattern from the CFM model matches well the location and trend of the Coyote Hills and Santa Fe Springs anticlines and the orientation of the central Los Angeles trough (Fig. 3b). Structural trend of these anticlines in the model changes from west- to northwest-trending along strike towards Santa Fe Springs, which is consistent with the trend of the folds in the subsurface and associated topography at the surface. A structural low in the model to the north of the anticlinal uplift (Fig. 3b) mimics the location of the La Habra syncline. In detail the La Habra syncline is being uplifted relative to the LA basin (Figs. 3a), an observation that is produced by the model as well. Model-data compatibility to the east of the San Gabriel River, therefore, is good and suggests that the CFM in this region is compatible with the observed fold structures. This result is particularly important because the Puente Hills thrust is well-constrained in the region of Santa Fe Springs by industry seismic data in the upper crust and by the hypocentral location of the Whittier Narrows earthquake mainshock (Shaw et al., 2002).

Comparison of model and data to the west of the San Gabriel River, in contrast, indicates that patterns of uplift from BEM models of the CFM do not match well geologically-constrained locations and orientations of major folds. In the region south of the Hollywood fault and east of the Newport-Inglewood fault, the model predicts that subsidence dominates the vertical motion (Fig. 3b). Geologically, this region marks the crest of the Elysian Park anticlinorium between the Las Cienegas monocline on the south and the Elysian Park anticline on the northeast (Figs. 1 and 3a). However, within the model, subsidence is produced over much of the area between the San Gabriel River and the Newport-Inglewood fault (Fig. 3b). Whereas the Elysian Park anticlinorium dominates the surface and subsurface deformation (Figs. 1 and 3a), the CFM-based model fails to produce uplift in this region (Fig. 3b). Improvement of the match between the model and geologic uplift patterns thus requires testing alternatives to the CFM fault configuration west of the San Gabriel River.

2. An integrated model with a steep Los Angeles segment of the Puente Hills thrust, rooting into lower Elysian Park thrust that extends from the San Gabriel to the northwest under the Santa Monica Mountains, and unlinking of the Raymond and Hollywood faults results in uplift rates and a pattern of uplift that departs from that of the CFM and approaches the geometry of the folds (Figs. 3a and 3c). A distinct monoclinial form to the model uplift rates is expressed in the western transect, C. Each of the major geologic features of the cross-section, including the LA trough and the limb and crest of the Las Cienegas monocline are reproduced in transect by model 5 (Fig. 3c). Likewise, the integrated model produces uplift

within the eastern transect, F, that is consistent with the geologic structure. Discrete anticlinal crests are created in the region of the Las Cienegas monocline on the south and the Elysian Park anticline on the north. The geologic data indicate the intervening region is characterized by consistently increasing structural relief and uplift rate (Fig. 3a), whereas the model uplift rate decrease and then increases from south to north across this region (Fig. 3c). Uplift rates from the model more closely approximate rates in the east on transect F than in the west on transect C. Whereas none of these modifications to the fault geometry affect the pattern of uplift in the Santa Fe Springs region to the east of the San Gabriel River, they do cause an overall increase in uplift rate (Fig. 3).

Marked improvement in model-data compatibility is also seen in map view (Fig. 3). A clearly defined northwest-trending region of subsidence is localized to the east of the Newport-Inglewood fault, which coincides well with the location of the central trough of the LA basin (Fig. 1). Some features of the Elysian Park anticlinorium are more clearly expressed in the composite model. A doubly-plunging west-northwest trending region of uplift, for example, develops to the south of the Raymond and Hollywood faults where the Elysian Park anticline occurs (Figs. 1, 3a, and 3c). Not clearly identifiable in the model, however, is the Las Cienegas monocline, which is a function of the difference in fold wavelength and geometry produced by BEM model faults. Uplift in the region of the Santa Fe and Coyote segments of the Puente Hills thrust system is higher and more laterally extensive in the integrated model than in the CFM. The model does show a structural low separating folds and faults in the east and west, respectively, which is a structural low reflected by the regional topography and the location of the San Gabriel River (Fig. 1). That these uplifts overlap in map view in the model implies that the Santa Fe Springs segment may be more laterally extensive in the CFM than is suggested by the well data.

Products

Cooke, M. L., and Marshall, S. T., 2006, Fault slip rates from three-dimensional models of the Los Angeles metropolitan area, California: *Geophysical Research Letters*, v. 33, L21313, doi:10.1029/2006GL027850.

Meigs, A., Cooke, M. L., and Marshall, S. T. (in review), Using vertical rock uplift patterns to infer and validate of three-dimensional fault configuration in the Los Angeles basin, *BSSA*.

Databases of vertical rock uplift rate for the R, P, and Q units have been contributed to the SCEC vertical motion database.

References

Argus, D., Heflin, M., Peltzer, G., Crampe F. and Webb, F. 2005. Interseismic strain accumulation and anthropogenic motion in metropolitan Los Angeles, *JGR*, doi:10.1029/2003JB002934.

Griffith, W.A. and Cooke, M.L., 2005. How sensitive are fault slip rates in the Los Angeles to tectonic boundary conditions? *BSSA*, vol. 95, pp. 1263-1275.

Shaw, J.H., Plesch, A., Dolan, J.F., Pratt, T.L., and Fiore, P., 2002, Puente Hills blind-thrust system, Los Angeles, California: *BSSA*, 92, p. 2946-2960.

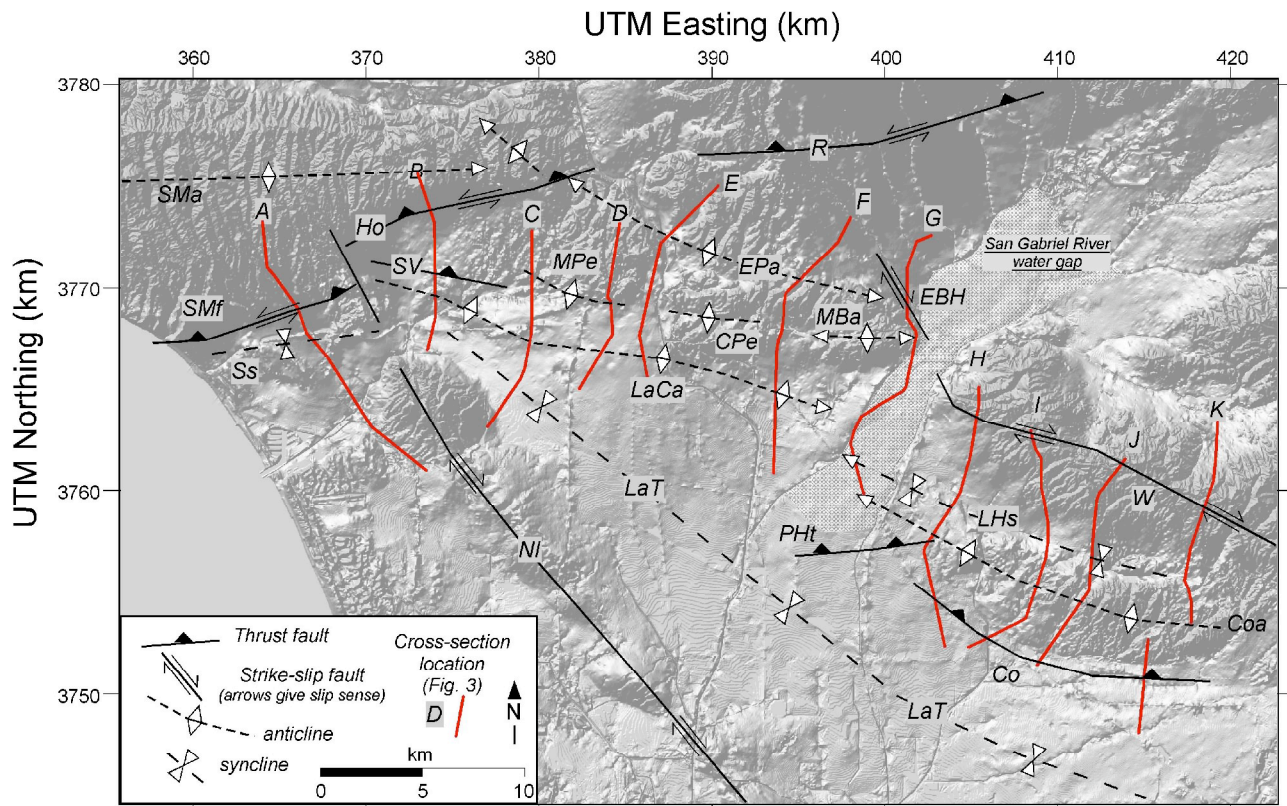


Figure 1 (above). Major structures in the northern Los Angeles basin are blind and emergent thrust faults and strike-slip faults in the boundary region between the east-west trending Transverse Ranges and northwest trending Peninsular Ranges structural provinces. Major thrust faults include the Raymond, Hollywood, Santa Monica, San Vincente (SV), Puente Hills blind thrust, and Coyote Hills blind thrust. Strike-slip faults include the Newport-Inglewood (NI), East Montebello Hills fault (EBH) and Whittier faults. Key folds include the Santa Monica Mountains Anticlinorium, the Elysian Park anticlinorium (EPa), the McArthur Park escarpment (Mpe), the Coyote Pass escarpment (CPe), the Montebello Hills anticline (Mba), the La Cienegas monocline, the Coyote anticline (Coa), the La Habra syncline (LHS), and the trough of the Los Angeles basin.

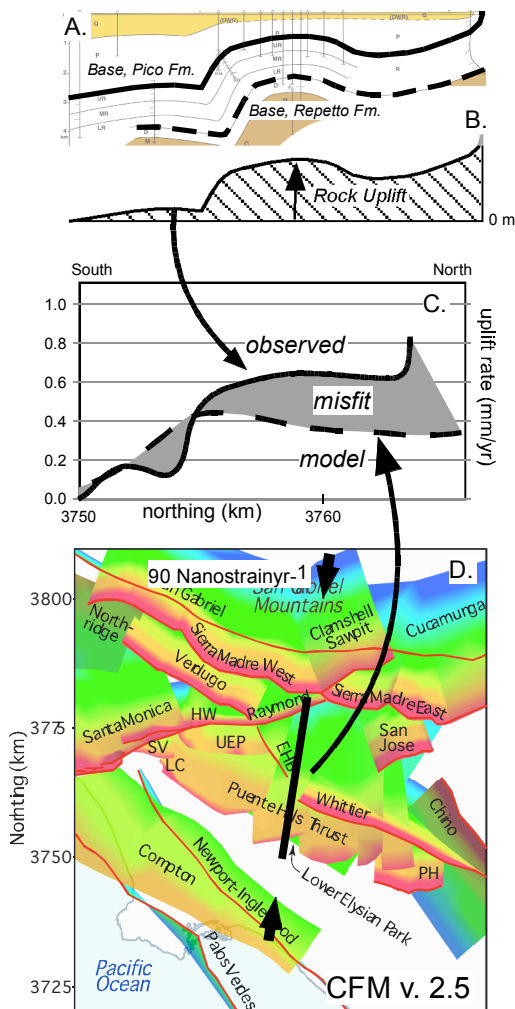


Figure 2 (left): Rock uplift rate and BEM model uplift rate integration. (A) Deformed stratigraphic markers (i.e. top or bottom contacts of stratigraphic formations) from cross sections are used to constrain marker depth across strike. (B) Rock uplift is inverted from depth by measuring marker structural relief relative to a reference depth. The greatest depths of a marker in a basin or at the center of a syncline represent potential choices for reference depths. (C) Rock uplift rate is the rock uplift divided by the age of the marker. (D) CFM fault surfaces within the Los Angeles basin color shaded to 27.5 km depth: warmer colors indicate shallower depths. Vertical faults are represented as red lines. Darker backlit surfaces are south-dipping. A regional shortening constrained by geodetic data is imposed on the model faults. Model uplift rate along a profile parallel to a geological cross-section (D) is extracted from the uplift rate field predicted by the model (C). Differences between measured and modeled uplift rate represent data-model misfit (C).

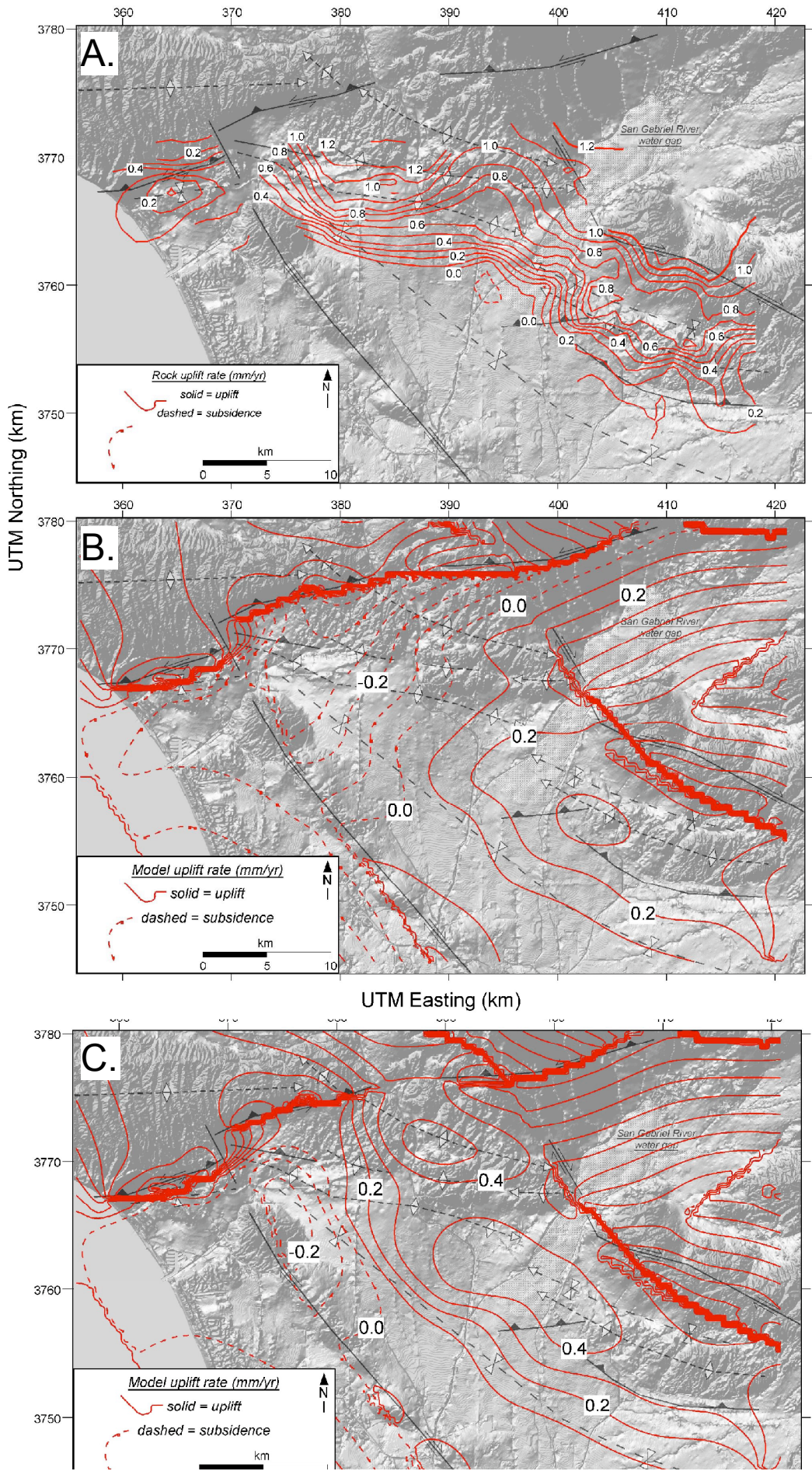


Figure 3. Rock uplift rate (A) inverted from the depth of the base of the Pico Member of the Fernando Formation along the northern shelf of the Los Angeles basin. Rock uplift represents the structural relief of the base relative to 3000 m at depth, which corresponds to the base of the Pico throughout the northern shelf. Rock uplift rate is the structural relief (A) divided by the age of the unit (Pico Member, Fernando Formation). The base of the Pico Formation is 2.9 Ma. Major structures defined in the Figure 2 caption. (B) Uplift and subsidence predicted from BEM of CFM v. 2.5 (C) Uplift and subsidence predicted from BEM of CFM v. 2.5, modified to the preferred model which includes steepening the Los Angeles fault to match the dip of the Las Cienegas fault, extending the lower Elysian Park ramp, and disconnecting the Raymond from the Hollywood faults. Major structures defined in the Figure 1 caption.